PERGAMON

Acta mater. 48 (2000) 2633–2638

Acta MATERIALIA

www.elsevier.com/locate/actamat

# PHASE REACTIONS IN THE Nb–N SYSTEM BELOW 1400°C

**W. LENGAUER[1]†, M. BOHN[2], B. WOLLEIN[1] and K. LISAK[3]**

[1]Institute for Chemical Technology of Inorganic Materials, Vienna University of Technology, Getreidemarkt 9/161, A-1060 Vienna, Austria, [2]CNRS-URA 6538, Centre de la Microsonde de l'Ouest, IFREMER, Centre de Brest, F-29280 Plouzané, France and [3]Department of Materials Technology, Austrian Research Centre Seibersdorf, A-2444 Seibersdorf, Austria

*(Received 8 December 1999; accepted 3 February 2000)*

**Abstract**—In continuation of a recent study on high-temperature nitridation of niobium the phase equilibria of the Nb–N system were investigated for $T \leq 1400°C$ by means of diffusion couples, electron probe microanalysis (EPMA) and differential scanning calorimetry (DSC). The $\gamma$-$Nb_4N_{3\pm x} \rightarrow \delta$-$NbN_{1-x}$ phase transition was investigated as a function of composition and occurs at temperatures between 1070°C (45.2 at.% N) and 1225°C (38.9 at.% N). The equilibrium composition of $\gamma$-$Nb_4N_{3\pm x}$ in this temperature interval is—depending on the temperature—only 42–44.0 at.% N, hence the transition occurs also in samples with a non-equilibrium composition. It can only be investigated by using *in situ* methods such as DSC and high-temperature X-ray diffraction because of the fast transition rate which does not permit quenching and which is responsible for the contradictory results in the literature. The congruent transformation $\eta$-NbN $\rightarrow \delta$-$NbN_{1-x}$ was observed between 1300 and 1320°C. Homogeneity ranges were measured from the phase bands of the diffusion couples by means of EPMA and the results are presented in the form of a phase diagram. © *2000 Acta Metallurgica Inc. Published by Elsevier Science Ltd. All rights reserved.*

*Keywords:* Electron microprobe analysis; Nitrides; Diffusion (bulk); Microstructure; Phase transformations (phase equilibria)

## 1. INTRODUCTION

The Nb–N system is interesting because of the superconducting behaviour of the $\delta$-$NbN_{1-x}$ phase and of its extension into ternary phases such as (Ti, Nb)$N_{1-x}$ [1]. Several different phase diagrams of the Nb–N system were proposed. Brauer and Esselborn [2] presented a nitrogen-rich portion in which at temperatures between 1280 and 1400°C a two-phase field $\gamma$-$Nb_4N_{3\pm x}$ + $\delta$-$NbN_{1-x}$ is shown, whereas at higher temperatures than 1400°C the $\gamma$-$Nb_4N_{3\pm x} \rightarrow \delta$-$NbN_{1-x}$ transition is—separated by a tricritical point from the two-phase field—of higher order (continuous transition without a two-phase field). Also a so-called $\delta'$-$NbN_{\approx 0.9}$ phase was introduced at $T = 1100$–1280°C. Guard *et al.* [3] investigated the nitrogen-rich portion by means of nitridation of compact Nb metal and did not find the $\delta'$-$NbN_{\approx 0.9}$ phase. Also their phase diagram does not contain the continuous transition between $\gamma$-$Nb_4N_{3\pm x}$ and $\delta$-$NbN_{1-x}$. The latter version was taken as a basis by Levinskii [4] who constructed a $p$–$T$–$x$ diagram from literature data. The version of Levinskii was adopted for the *Handbook of Binary Alloy Phase Diagrams* [5], but the $\delta$-$NbN_{1-x}$ phase designation was omitted. Brauer and Kern [6] also presented a phase diagram, together with detailed information on nitrogen equilibrium pressures—in which a continuous $\gamma \rightarrow \delta$ transition at *c.* 1400°C as well as a two-phase field was introduced again.

From these studies it appears that the phases $\beta$-$Nb_2N$, $\gamma$-$Nb_4N_{3\pm x}$, $\delta$-$NbN_{1-x}$ and $\eta$-NbN can be considered as stable phases, whereas the $\delta'$-$NbN_{\approx 0.9}$ phase seems to occur only transiently in the formation of $\eta$-NbN from $\delta$-$NbN_{1-x}$. Recently, a calculation of the phase equilibria was reported [7] but neither $\gamma$-$Nb_4N_{3\pm x}$ nor $\eta$-NbN was included because they were assumed to be oxygen stabilized. This is definitely not the case if the above-cited experimental studies are taken into consideration.

Although a lot of effort has been undertaken for the clarification of the Nb–N system a satisfactory and unambiguous level of knowledge on the phase reactions has not been attained and the various proposed phase diagrams [2–8] are contradictory. This is especially true for the phase reactions in which $\gamma$-$Nb_4N_{3\pm x}$ is involved. The reason for the most part of this contradiction is the fast rate of $\gamma$-$Nb_4N_{3\pm x}$ phase formation from $\delta$-$NbN_{1-x}$ which requires *in*

† To whom all correspondence should be addressed.


PII: S1359-6454(00)00056-2

*situ* investigation techniques, which was shown recently by application of high-temperature X-ray diffraction [9]. In addition, studies with compact sample material permit insight of the thermal history by inspection of their microstructures. Thus valuable information for the phase equilibria can be obtained even if some transition occurs between high-temperature annealing and ambient-temperature investigations.

In order to clarify the most controversial region in this system, diffusion couples, some of which were of wedge-type geometry, and DSC investigations were performed in the present study. Advantages of wedge-type diffusion couples have been outlined elsewhere (e.g. Ref. [10]).

## 2. EXPERIMENTAL

### 2.1. DC technique

Diffusion couples of various shapes were annealed in high-purity nitrogen of various pressures, times and temperatures. The starting material was 99.9 wt% Nb. Especially at the low temperature region of the present investigation annealing periods up to 2 weeks were necessary in order to obtain phase band thicknesses accessible for light optical microscopy.

### 2.2. DSC

Differential scanning calorimetry was made in a Netzsch DSC 404 calorimeter at heating rates of 5, 10 and 20 K/min in purified Ar (activated Cu, 99.999 vol.% Ar) using a Pt crucible. A thin sapphire disc was put between the sample and the crucible in order to avoid reaction of the sample with Pt. Standardization was performed by using five certified metal standards In, Sn, Al, Au and Ni of which the melting temperature was fitted by a polynomial expression. The error in temperature is less than 0.5%.

The samples were made of nitrided Nb sheet of various thickness up to 1 mm. Different nitrogen contents were adjusted by establishing appropriate temperatures and nitrogen pressures for prolonged annealing times [11] in order to obtain homogeneous samples. The samples were measured by GC-Dumas for their nitrogen content.

The sheets were lapped on one side in order to guarantee good contact with the sapphire disk in the crucible for optimum heat flow. Plates of 3 mm in diameter were prepared from the lapped sheets with a hollow drill bit.

### 2.3. Electron probe microanalysis

Electron probe microanalysis (EPMA) was carried out with wavelength-dispersive spectrometers (using a W/Si multilayer crystal for nitrogen) and application of niobium nitride standards, which were chemically analysed for nitrogen, carbon (GC-Dumas), oxygen (hot extraction) and niobium (combustion in air). The EPMA conditions were optimized to a level where independent measurements on the same samples performed over more than one year yielded a difference of a few tenths at.% N only. Details are given elsewhere [12].

## 3. RESULTS AND DISCUSSION

### 3.1. Formation of the $\gamma$-$Nb_4N_{3\pm x}$ phase

The microstructure of the phase band of the $\delta$-$NbN_{1-x}+\gamma$-$Nb_4N_{3\pm x}$ phases formed in a temperature region around 1350°C where, according to the literature [2, 3], $\delta$-$NbN_{1-x}$ and $\gamma$-$Nb_4N_{3\pm x}$ should coexist, is characterized by a hatched microstructure at the $\gamma$-$Nb_4N_{3\pm x}$ inner side which continuously fades into the $\delta$-$NbN_{1-x}$ outer side (Fig. 1). The absence of a metallographically visible clear interface between these two phases in diffusion couples is representative of the absence of a two-phase field. Figure 2 shows that the nitrogen profile within this region is smooth. If the composition of $\gamma$-$Nb_4N_{3\pm x}$ is different from $\delta$-$NbN_{1-x}$ due to a two-phase field then a much more scattered profile would occur especially at the position where $\gamma$-$Nb_4N_{3\pm x}$ and $\delta$-$NbN_{1-x}$ merge into each other.

In a previous study [9] high-temperature X-ray diffraction measurements (HTXRD) yielded that this transition is reversible and occurs actually around a temperature of 1120°C—much lower than reported in the literature. However, measurements of the transition temperature as a function of composition could not be performed by HTXRD because the measurements were applied on $\delta$-

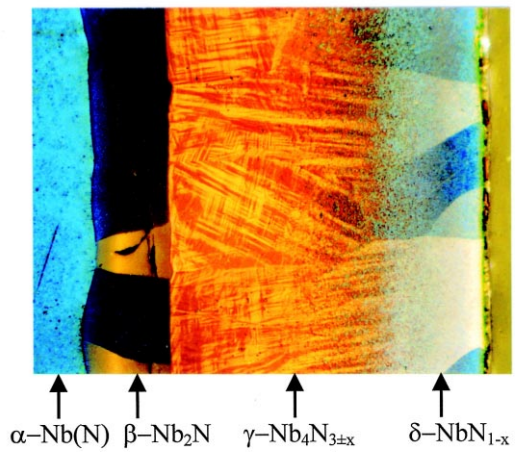


Fig. 1. Microstructure of a diffusion couple annealed at $T = 1350$°C. The hatched structure is due to the formation of $\gamma$-$Nb_4N_{3\pm x}$ which fades into the $\delta$-$NbN_{1-x}$ phase. Anodically oxidized, polarized light, makes the hatching of the $\gamma$-$Nb_4N_{3\pm x}$ phase visible.

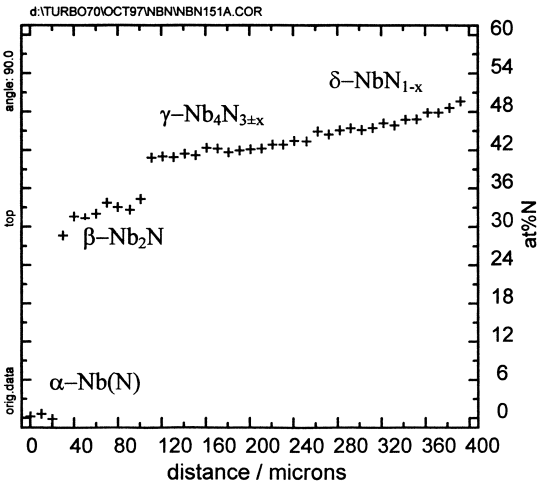


Fig. 2. EPMA line scan showing a smooth variation of the nitrogen profile in the $\gamma$-$Nb_4N_{3\pm x}$ + $\delta$-$NbN_{1-x}$ phase field.

$NbN_{1-x}$/$\gamma$-$Nb_4N_{3\pm x}$ diffusion layers made by heating Nb strips within the HTXRD chamber (at appropriate temperature and nitrogen pressure conditions suitable for preparing a nitrogen-poor $\delta$-$NbN_{1-x}$) and by subsequent investigation by diffraction without cooling to room temperature. This was made in order to guarantee high-purity *in situ* conditions. The investigated phase band is inhomogeneous in composition by nature and because of the penetration depth of X-rays of several micrometres the transition seen from a diffusion layer cannot be attributed to a single composition.

Thus homogeneous samples were prepared and subjected to differential scanning calorimetry (DSC). The $C_p$ curve of a transition between $\gamma$-$Nb_4N_{3\pm x}$ and $\delta$-$NbN_{1-x}$ is shown in Fig. 3. The integration of $C_p$ yields 3.6 kJ/mol for the heating cycle and 4.0 kJ/mol for the cooling cycle, where 1 mol refers to $NbN_{0.672}$ which is 102.33 g. DSC investigations of samples different in compositions within a narrow compositional region resulted in a drop in transition temperature upon increasing nitrogen content (Fig. 4). A transition could be observed by DSC even if the $\delta$-$NbN_{1-x}$/$\gamma$-$Nb_4N_{3\pm x}$ samples had a nitrogen content lower or higher than corresponding to the equilibrium composition of $\gamma$-$Nb_4N_{3\pm x}$ (the preparation of nitrogen-poor $\delta$-$NbN_{1-x}$ is possible because at high temperatures the nitrogen-poor phase boundary bends towards Nb; upon cooling it transforms to $\gamma$-$Nb_4N_{3\pm x}$). Therefore, in Fig. 4 transitions are indicated also below and above the given homogeneity range of $\delta$-$NbN_{1-x}$/$\gamma$-$Nb_4N_{3\pm x}$ at 1100–1300°C. From these DSC results it can be concluded that the transformation into $\gamma$-$Nb_4N_{3\pm x}$ as shown in Fig. 1 occurs on the nitrogen-poor side of $\delta$-$NbN_{1-x}$ upon cooling.

Different heating/cooling rates interestingly showed an increasing hysteresis in temperature upon increasing heating rate. The increase is caused by the shift of the transition temperature of the reaction $\delta$-$NbN_{1-x} \rightarrow \gamma$-$Nb_4N_{3\pm x}$ (cooling) and not upon the reverse reaction $\gamma$-$Nb_4N_{3\pm x} \rightarrow \delta$-$NbN_{1-x}$ (heating), see Fig. 5. Obviously, the lattice distortion caused by the formation of the tetragonal $\gamma$-$Nb_4N_{3\pm x}$ phase upon cooling creates stresses which are overcome only within some time (compare the hatched microstructure in Fig. 1). For the reverse transformation no lattice distortion occurs with the formation of the f.c.c. $\delta$-$NbN_{1-x}$ and the transformation remains at the same temperature irrespective of the heating rate.

Several diffusion couple annealings were made within the temperature range where the $\delta$-$NbN_{1-x} \rightarrow \gamma$-$Nb_4N_{3\pm x}$ transformation occurred. An interface caused by a compositional discontinu-

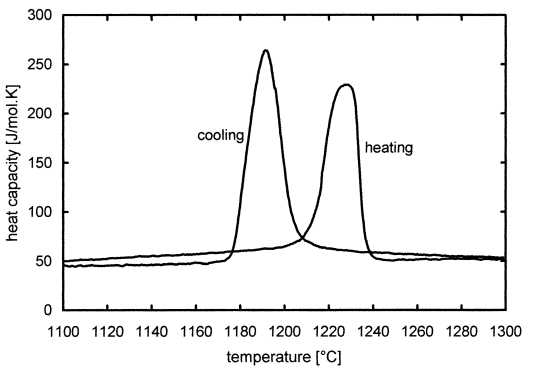


Fig. 3. $C_p$ of the transformation $\gamma$-$Nb_4N_{3\pm x} \rightarrow \delta$-$NbN_{1-x}$ upon heating and on the reverse reaction $\delta$-$NbN_{1-x} \rightarrow \gamma$-$Nb_4N_{3\pm x}$ for 102.33 g (1 mol) of $NbN_{0.672}$. Sample composition 40.2 at.% N.

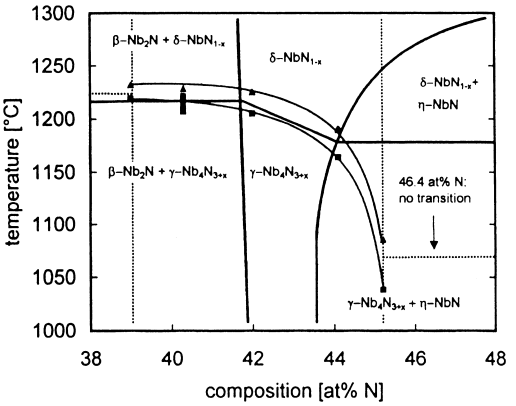


Fig. 4. Results on the $\gamma$-$Nb_4N_{3\pm x} \rightarrow \delta$-$NbN_{1-x}$ transformation as a function of composition (partial Nb–N phase diagram). Triangles: heating cycle ($\gamma$-$Nb_4N_{3\pm x} \rightarrow \delta$-$NbN_{1-x}$), squares: cooling cycle ($\delta$-$NbN_{1-x} \rightarrow \gamma$-$Nb_4N_{3\pm x}$). The solid phase field lines represent the equilibrium phase diagram, the dotted lines the non-equilibrium situation because samples with lower or higher nitrogen content than given by the equilibrium phase boundaries also showed a transition. In samples annealed at 1100°C a homogeneity range of 41.9–43.4 at.% N was measured for the $\gamma$-$Nb_4N_{3\pm x}$ phase.

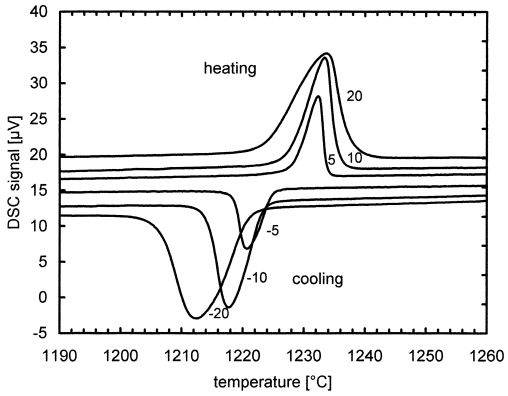


Fig. 5. Heating/cooling cycles with different heating and cooling rates (the numbers give the rates in K/min). Top: heating ($\gamma$-$Nb_4N_{3\pm x} \rightarrow \delta$-$NbN_{1-x}$), bottom: cooling ($\delta$-$NbN_{1-x} \rightarrow \gamma$-$Nb_4N_{3\pm x}$). Upon cooling the temperature of the reaction $\delta$-$NbN_{1-x} \rightarrow \gamma$-$Nb_4N_{3\pm x}$ shifts to lower temperatures the higher the cooling rate. This is due to the formation of the tetragonal $\gamma$-$Nb_4N_{3\pm x}$ which causes stress because of lattice deformation.

ity within the $\gamma$-$Nb_4N_{3\pm x}$ + $\delta$-$NbN_{1-x}$ phase band should be metallographically visible if a two-phase field $\gamma$-$Nb_4N_{3\pm x}$ + $\delta$-$NbN_{1-x}$ was present at the annealing temperature. In order not to overlook the presence of an interface due to a first-order reaction occurring in some small temperature region a temperature-gradient diffusion couple (cf. Ref. [13]) was used one end of which was held at 1170°C and the other at 1300°C. Again no interface could be detected. Thus it can be concluded that a two-phase field between $\gamma$-$Nb_4N_{3\pm x}$ and $\delta$-$NbN_{1-x}$ is absent and the $\gamma$-$Nb_4N_{3\pm x}/\delta$-$NbN_{1-x}$ transformation is quasi continuous.

The structures of both phases are so closely related [14] that upon transformation of one structure into the other the nitrogen atoms have to jump only over very small distances, presumably only to next-neighbour positions. The Nb sublattice behaves like in a martensitic transition, characteristic of a change in the lattice axes only. Hence this transition cannot be quenched and *in situ* investigation methods have to be applied to find the transition temperature.

### 3.2. *η-NbN phase formation*

Wedge-type diffusion couples annealed in the temperature range of 1100–1400°C were inspected at the outermost region where the $\eta$-NbN phase should form. At the low temperature end the diffusion of nitrogen in the various phases is so slow that annealing cycles of several weeks were necessary in order to obtain diffusion layers suitable for investigation in the light-optical microscope and especially by means of electron probe microanalysis

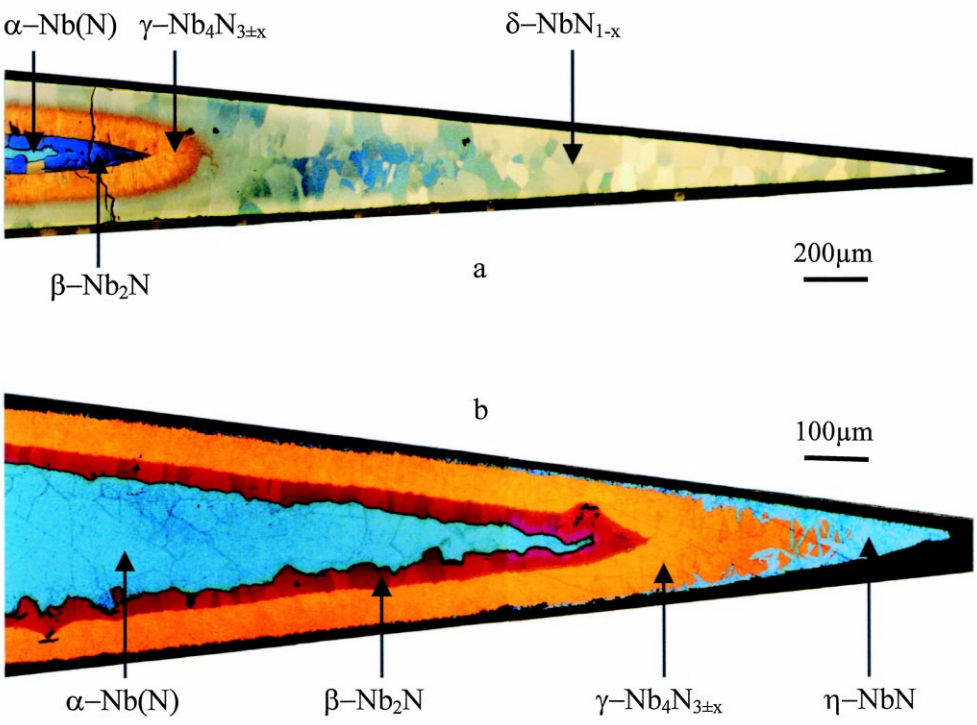


Fig. 6. Microstructures of a wedge-type diffusion couple annealed above (a) and below (b) the decomposition temperature of $\eta$-NbN. Note the thickness enhancement of the $\eta$-NbN phase band at the tip. Anodically oxidized. Polarized light used for (a). In sample (a) the inner (yellow–brown) part of the $\delta$-$NbN_{1-x}$ phase transformed into $\gamma$-$Nb_4N_{3\pm x}$ upon cooling.

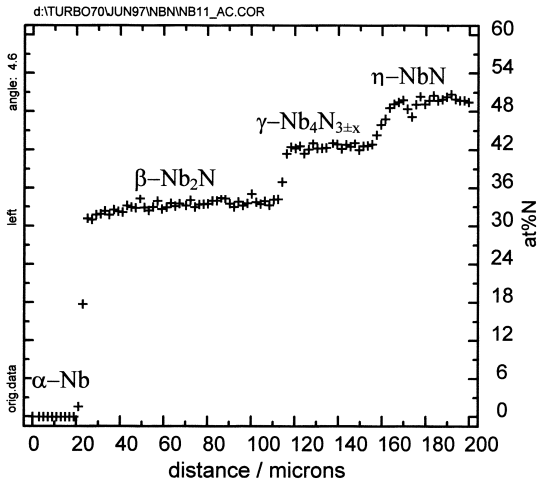


Fig. 7. EPMA line scan along the symmetry axis of a wedge-type diffusion couple of the type shown in Fig. 6(b) ($\eta$-NbN phase present).

which requires thicknesses of at least about 10 μm in order to measure concentration profiles.

By means of wedge-type diffusion couples the presence or absence of the $\eta$-NbN phase could be unambiguously seen because this phase thickens considerably towards the tip. It is hardly detectable at larger sample thicknesses or in plane-sheet samples of large thickness if the annealing time is too short. Thus it can be overlooked and concluded to be not stable at a given annealing temperature. In addition, thicker phase bands could be characterized by measuring the nitrogen profile by EPMA and thus the homogeneity ranges.

A wedge-type sample in which the $\eta$-NbN phase is absent also at the tip because of thermodynamic instability is shown in Fig. 6(a) where the $\delta$-$NbN_{1-x}$ phase extends to the surface (an EPMA scan of such a sample type is given in Fig. 2). Contrary, in the microstructure of the sample shown in Fig. 6(b) the $\eta$-NbN phase is clearly visible at the near-tip positions of the wedge-type sample. A corresponding EPMA scan of a sample in which the $\eta$-NbN was stable at the annealing temperature is shown in Fig. 7. This scan was recorded in the symmetry plane of a wedge-type sample in order to further increase the number of data points. From the metallographic investigation of such samples the stability temperature of $\eta$-NbN could be found to be located between 1300 ($\eta$-NbN present) and 1320°C ($\eta$-NbN absent).

### 3.3. Phase diagram for the Nb–N system

From the DSC, metallography and EPMA, a phase diagram of the Nb–N system was drawn (Fig. 8) in which also the high-temperature results of a previous study were introduced for completeness. Thus it is representative for nitrogen equilibrium pressures $\leq 30$ bar $N_2$.

The broken line in the area of the $\gamma$-$Nb_4N_{3\pm x} \rightarrow \delta$-$NbN_{1-x}$ phase transition represents also the results of the samples which had a non-equilibrium composition at the investigation temperatures. The solid lines in this region give the transition for the equilibrium samples (cf. also Fig. 4). For this the midpoints of temperatures of the heating and cooling cycles were used.

Microprobe line scans of all wedge-type samples showed that upon increasing temperature the $\delta$-$NbN_{1-x} + \eta$-NbN two-phase region narrows down until the $\delta$-$NbN_{1-x}$ phase attains the same composition as $\eta$-NbN and the congruent reaction between $\eta$-NbN and $\delta$-$NbN_{1-x}$ takes place.

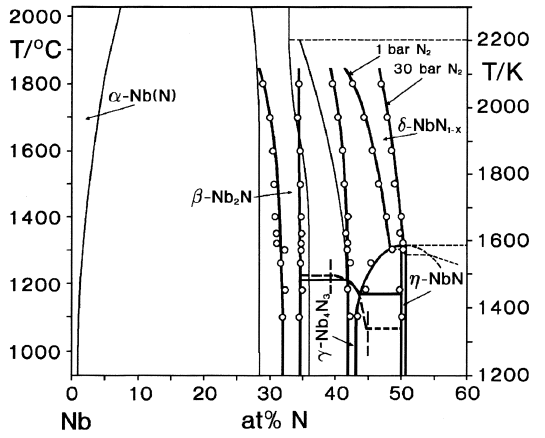


Fig. 8. Phase diagram of the Nb–N system from results of the present study together with high-temperature data of a previous study [11]. The thin lines are from Ref. [8]. The broken line represents the non-equilibrium $\delta$-$NbN_{1-x}/\gamma$-$Nb_4N_{3\pm x}$ transition (midpoints of the heating and cooling cycles), for the equilibrium portion see Fig. 4.

## 4. CONCLUSION

The region below 1400°C of the Nb–N system, most controversially reported in the literature, was investigated by diffusion couples and compact samples. This has several advantages over powder samples used in the past because also metallographic inspection and electron probe microanalysis is possible. The $\gamma$-$Nb_4N_{3\pm x} \rightarrow \delta$-$NbN_{1-x}$ transition could be characterized to be of quasi continuous nature (absence of a two-phase field). This could not be performed by powder samples and the findings from such sample material were misinterpreted [2, 6].

Also the decomposition temperature of $\eta$-NbN was obtained and the measurement of the homogeneity ranges of all phases stable in the temperature range 1100–1400°C was performed. In combination with the high-temperature data from a previous study [9] the phase diagram of the Nb–N system up to 50 at.% N could be established.

*Acknowledgements*—The authors would like to thank Mr Meinrad J. Ostermann, Teledyne Metalworking Products, Huntsville, AL, for supplying various refractory metals. This work was supported by the Austrian Science Foundation FWF, project 11178 and by the French–Austrian Scientific-Technical Cooperation AMADEUS, project 10j.

## REFERENCES

1. Mayr, W., Lengauer, W., Buscaglia, V., Bauer, J., Bohn, M. and Fialin, J., *J. Alloys Comp*., 1997, **262–263**, 521.
2. Brauer, G. and Esselborn, R., *Z. anorg. anorg. Chem*., 1961, **309**, 151.
3. Guard, R., Sawage, J. and Swarthout, D., *Trans. metall. Soc. A.I.M.E*., 1967, **239**, 643.
4. Levinskii, Y. V., *Izv. Akad. Nauk SSSR, Metal*., 1975, **1**, 52.
5. Massalski, T. B. (ed.), *Handbook of Binary Alloy Phase Diagrams*, CD-ROM edn. ASM, Materials Park, OH, 1995.
6. Brauer, G. and Kern, W., *Z. anorg. allg. Chem*., 1983, **597**, 127.
7. Huang, W., *Metall. Mater. Trans. A*, 1996, **27A**, 3591.
8. Politis, C. and Rejman, G., Kernforschungszentrum Karlsruhe (Germany). Report No. KfK-Ext. 6/78-1, 1978.
9. Berger, R., Lengauer, W. and Ettmayer, P., *J. Alloys Comp*., 1997, **259**, L9.
10. Wiesenberger, H., Lengauer, W. and Ettmayer, P., *Acta mater*., 1998, **46**(2), 651.
11. Joguet, M., Lengauer, W., Bohn, M. and Bauer, J., *J. Alloys Comp*., 1998, **269**, 233.
12. Lengauer, W., Bauer, J., Bohn, M., Wiesenberger, H. and Ettmayer, P., *Mikrochim. Acta*, 1997, **126**, 279.
13. Lengauer, W., *Acta metall. mater*., 1991, **39**(12), 2985.
14. Christensen, A. N., Hazell, R. G. and Lehmann, M. S., *Acta chem. scand. A*, 1981, **35**, 111.